AIP | Applied Physics Letters

Differentiation of topographical and chemical structures using an interfacial force microscope

Stephen A. Joyce, J. E. Houston, and T. A. Michalske

Citation: Applied Physics Letters **60**, 1175 (1992); doi: 10.1063/1.107396
View online: http://dx.doi.org/10.1063/1.107396
View Table of Contents: http://scitation.aip.org/content/aip/journal/apl/60/10?ver=pdfcov
Published by the AIP Publishing

Articles you may be interested in

Evidence for the formation of ordered layers on SeS2 treated GaAs(110) using atomic force microscopy
J. Appl. Phys. **80**, 6274 (1996); 10.1063/1.363703

Study of thin organic overlayers by local probe microscopies
AIP Conf. Proc. **354**, 364 (1996); 10.1063/1.49491

Electrontopological approach to computeraided molecular design in QSAR problems: An experience of development and use
AIP Conf. Proc. **330**, 631 (1995); 10.1063/1.47811

Computer generation of chemical structures using the gem program
AIP Conf. Proc. **330**, 544 (1995); 10.1063/1.47757

Measurement of nanomechanical properties of metals using the atomic force microscope
J. Vac. Sci. Technol. B **12**, 2211 (1994); 10.1116/1.587743

This article is copyrighted as indicated in the article. Reuse of AIP content is subject to the terms at: http://scitation.aip.org/termsconditions. Downloaded to IP: 129.22.67.107 On: Mon, 24 Nov 2014 07:35:14

Differentiation of topographical and chemical structures using an interfacial force microscope

Stephen A. Joyce, J. E. Houston, and T. A. Michalske
Sandia National Laboratories, Albuquerque, New Mexico 87185

(Received 30 September 1991; accepted for publication 6 January 1992)

The forces between a tungsten tip and a self-assembled monolayer of hexadecylthiol ($C_{16}H_{33}SH$) on a thin gold film have been studied using a newly developed interfacial-force microscope. Imaging of the surface, combined with spatially resolved force versus separation measurements, allow for the distinction of topographical and chemical features of the surface. Several distinct regions are observed for this system. The first, characterized by a very weak interfacial interaction between tip and sample, is representative of the self-assembled monolayer. The other regions show relatively strong, long-range attractive forces, which are associated with gross defects in the film.

The atomic force microscope (AFM) has recently been used to image the microscopic, three-dimensional structure of a large number of both insulating and conducting samples.[1,2] The imaging is generally accomplished by scanning a sharp tip across a surface while maintaining a constant force (or force gradient) between tip and sample. For a homogeneous surface, such measurements reflect the topography of the sample. In addition, one can measure the force between the tip and sample at a fixed location as a function of the tip-sample separation. These force-separation profiles are a direct measure of the interfacial interaction and, as such, depend on the detailed chemical or material natures of both the tip and substrate surfaces. Combining both capabilities, imaging and force-separation profiles, allows the differentiation of the morphological and chemical features of heterogeneous samples. In this letter, we present such a study using the recently developed interfacial force microscope (IFM) to image the surface and measure selected area force-separation profiles for a tungsten (W) tip interacting with a self-assembled monolayer of hexadecylthiol ($C_{16}H_{33}SH$) adsorbed on a thin gold film. We find several regions on these surfaces: one is associated with "flat" areas characteristic of the self-assembled monolayer; the others are associated with gross defects in the Au-substrate film and with contaminants on the Au-film surface.

Self-assembled monolayers of organic molecules have recently been the focus of a considerable research effort due to their many unique properties and potential applications including, for example, use as nonlinear optical devices and electrochemical sensors.[3] For the present study, we have used an *n*-alkyl thiol, hexadecylthiol, adsorbed on a thin gold film. The thiol end group strongly chemisorbs on Au surfaces, while the normal alkyl backbone interacts with neighboring molecules through long-range van der Waals forces to form densely packed, ordered films.[4] The ideal result is a uniformly thick film ($\sim$25 Å) terminated with methyl groups. For this work, the thiol was deposited from a solution ($\sim$1 mM in ethanol) onto a thin ($\sim$100 nm) gold film which in turn had been deposited onto a silicon substrate. The substrates have a thin native-oxide layer and an intermediate thiolated silane layer is used to enhance the adhesion of the gold film.[5]

The interfacial force microscope has been described in detail elsewhere and will be discussed only briefly here.[6] Of primary importance to the present work is the ability to measure the interfacial-force profiles, i.e., the force between the tip and surface over the entire range of interfacial separations, from nanometers up to repulsive contact. Conventional cantilever-based force microscopes are not ideally suited for such measurements since they are mechanically unstable when the attractive force gradient between tip and sample exceeds the cantilever-force constant. This instability results in the discontinuous movement of the tip into contact with the sample. This "jump-to-contact" phenomenon has been observed frequently and described in detail by others.[7,8] The instability prevents the measurement of interfacial forces over the range of separations necessary to fully characterize the interfacial interaction.

We have developed a zero-deflection/force-feedback controlled IFM that does not suffer from the "jumping" behavior.[6] The mechanical instability is avoided by externally balancing the interfacial force so that the sensor deflection is minimized. The heart of the microscope is the differential capacitance-displacement sensor. A common capacitor plate, suspended on torsion arms about which it is free to rotate, is mounted above two fixed capacitor pads. When a sample is brought into the vicinity of a tip mounted on one end of the common plate, the interfacial force causes the deflection of the common plate. The resultant differential-capacitance change is detected by configuring the sensor as an ac impedance bridge. At this level, the unit can be operated as a conventional AFM. Force balancing can be achieved through the application of dc control voltages to the fixed-capacitor pads. The restoring force is of the form $F_r = -F_i = 2CV\Delta V/d$, where F_i is the interfacial force, V is a constant bias voltage applied to both fixed-capacitor pads, d is the capacitor gap, and ΔV is the control voltage. ($+\Delta V$ is applied to one pad, $-\Delta V$ to

 0003-6951/92/101175-03$03.00 © 1992 American Institute of Physics

This article is copyrighted as indicated in the article. Reuse of AIP content is subject to the terms at: http://scitation.aip.org/termsconditions. Downloaded to IP: 129.22.67.107 On: Mon, 24 Nov 2014 07:35:14

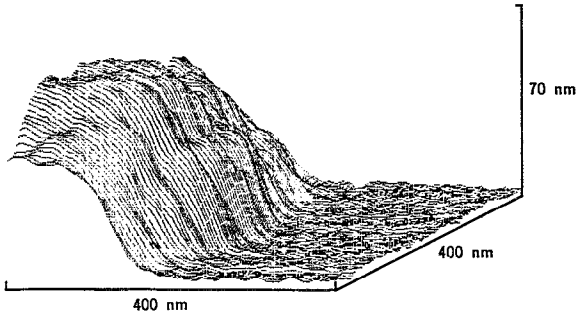

FIG. 1. Constant repulsive-force image of the self-assembled monolayer sample showing the edge of a large-scale defect.

the other.) Small, second-order corrections [of order $C(\Delta V)^2/d$] in the calculation of F_r are necessary when $C_1 \neq C_2$.

An electrolytically etched W tip[9] was attached to one end of the sensor using silver epoxy. Since the tip is exposed to air, it is presumably covered with a thin-oxide film. The samples were mounted to the end of a quadrant piezoelectric-tube scanner. Two modes of operation are commonly employed. For imaging, the feedback control to the sensor is turned off and a second feedback controller for the piezotube is used to image the surface at a constant repulsive force of $\sim 2 \times 10^{-7}$ N. For the selected-area force-profile measurements, the piezotube feedback controller is turned off and the sensor feedback on while the sample is scanned from ~ 60 nm separation to repulsive contact and then back out. The interfacial force is measured both upon approach and withdrawal. The experiments were carried out both in air and in a turbomolecular-pumped vacuum system. No significant differences between air and vacuum operation were observed.

Figure 1 shows a constant repulsive-force image of a self-assembled monolayer on a thin gold film. The 400 nm by 400 nm image reveals two relatively smooth areas (features up to a few nanometers high) separated by a 50-nm-wide step which is ~ 70 nm high. (As we will discuss later, this step is associated with defects in the substrate metallization.) The force images associated with such large-scale features are a convolution of the topographies of both the tip and sample. When the sample mount is physically moved so that other areas can be imaged, such large-scale features are observed about 20%–30% of the time. Smaller-scale protrusions (~ 100 nm diam, 10–30 nm high) are occasionally observed, while the remainder of the surveys show relatively flat surfaces over the entire image.

In order to better characterize these surfaces, force-profile measurements were performed over selected areas to determine whether any chemical effects are associated with the large-scale defects. Two such results are shown in Fig. 2 for areas above and below one of the large steps. Curve A in Fig. 2 is representative of the force measurements observed for the high regions above the steps. Note the absence of any strong, attractive forces between tip and sample upon approach. This behavior is consistent with the interaction of a metal tip and a chemically inert, hydrophobic surface such as the methyl-terminated self-assembled monolayer. The lack of any attractive forces upon withdrawal indicates the monolayer prevents adhesion between the tip and substrate even after repulsive-contact loading. The repulsive portions of the force profiles reflect both the elastic properties of the films and the compliance of the sensor. The hysteresis in the repulsive-force profiles is reproducible and corresponds to an anelastic response of the film.[10]

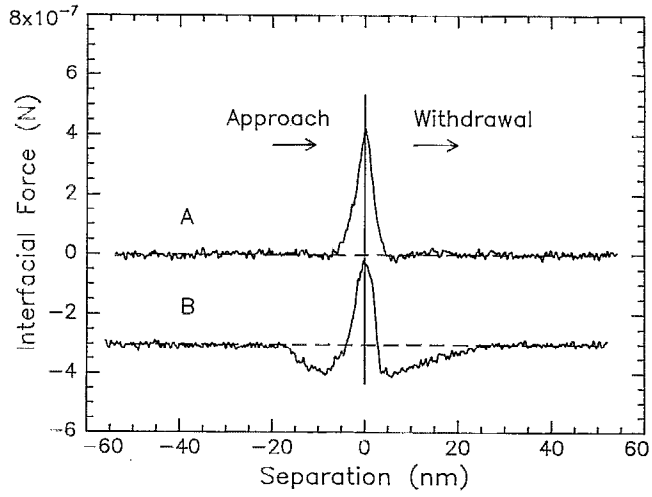

FIG. 2. Force-separation profiles from two areas near a defect. Negative separations refer to the distance between tip and sample on approach; positive separation indicates withdrawal. Attractive forces are negative, repulsive are positive. (A) Profile from the higher regions above the step. (B) Profile from the lower regions below the step.

As shown of Fig. 2(B), strikingly different force profiles are observed for the low regions adjacent to the steps. Strong, long-range attractive forces are seen. The attractive forces are longer range upon withdrawal, indicating a significant level of hysteresis. This behavior has been observed frequently and has been ascribed to capillary or meniscus forces between tip and sample.[11–13] Fluid layers on the surface or tip result in attractive forces by the formation of a meniscus when the tip and sample are brought into initial contact. Upon withdrawal, the attractive forces remain until the meniscus breaks. While the exact nature of the fluid layer responsible for these forces is not known, it is presumably some form of adventitious contaminant such as water and/or hydrocarbons. It is not unlikely, however, that the hydrophobic self-assembled monolayer would support such an interaction, suggesting that this region is not covered by the monolayer.

Similar measurements were performed on other areas of the samples. For the large-step defects, force profiles from the upper regions are usually characterized by weak attraction, representative of the self-assembled monolayer, while for the lower regions, contaminant meniscus forces are seen. At the smaller protrusions, similar behavior is observed, except that here the meniscus forces are usually found at the protrusion and the weak forces on the lower "flat" regions.

Using the correlation of the type of defects observed

This article is copyrighted as indicated in the article. Reuse of AIP content is subject to the terms at: http://scitation.aip.org/termsconditions. Downloaded to IP: 129.22.67.107 On: Mon, 24 Nov 2014 07:35:14

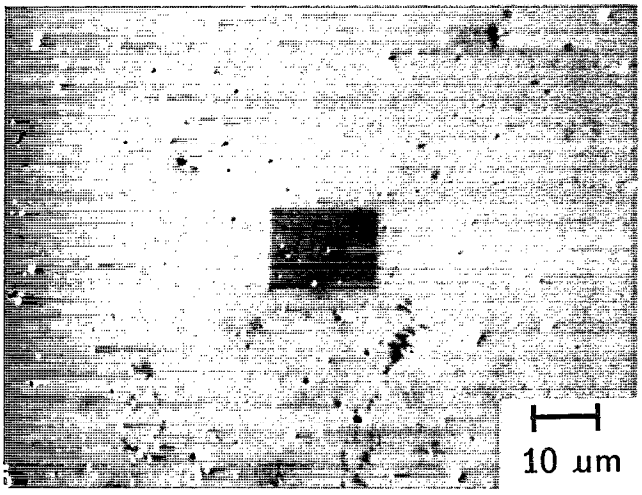

FIG. 3. SEM image of one of the samples. The darker rectangles in the center represent areas where the organic layer has been damaged by the larger electron-current densities used for high-magnification imaging.

during imaging and the associated force profiles, a simple picture of these surfaces can be drawn. Given that the height of the steps is about the nominal thickness of the Au film, these features most likely represent areas where gold was not deposited on the silicon substrate, perhaps due to contamination present during the Au deposition. The protrusions are presumably microscopic particles that adhered to the surfaces and either prevent thiol adsorption or simply cover the self-assembled monolayer.

Ultrahigh-vacuum scanning electron and scanning Auger microscopies (SEM) and (SAM) were performed to confirm the nature of the defects on these samples. A representative SEM image is shown in Fig. 3. Again, several distinct regions were observed. These regions consist principally of a featureless surface upon which dark circular and small bright features are observed. Selected-area Auger electron analysis shows that the majority of the surface is gold covered with carbon. The larger dark areas consist, however, of silicon with significant amounts of carbon and oxygen, while the bright areas are predominantly carbonaceous with traces of oxygen and gold.

In conclusion, we have characterized the topographical and chemical nature of a self-assembled monolayer adsorbed on a gold film using interfacial force microscopy. Imaging reveals a number of large-scale defects; selected-area force profiles show a chemically distinct nature of the sample in the vicinity of the defects. Over the majority of the surface, only weak interactions between tip and sample were observed, indicative of the low-energy surface produced by the self-assembled monolayer. Contaminant-related meniscus forces are associated with defects, i.e., areas not covered by the monolayer. This work has demonstrated the importance and utility of combining the imaging and force profiling capabilities of force microscopy for differentiating the microscopic structure and chemical nature of heterogeneous samples.

The authors thank Professor R. Crooks (UNM) for providing the films and for many helpful discussions and R. Wayne Buttry (SNL) for performing the SEM and SAM analysis.

[1] G. Binnig, C. F. Quate, and C. Gerber, Phys. Rev. Lett. **56**, 930 (1986).
[2] D. Sarid, *Scanning Force Microscopy* (Oxford University, New York, 1991).
[3] J. D. Swalen, D. L. Allara, J. D. Andrade, E. A. Chandross, S. Garoff, J. Israelachvili, T. J. McCarthy, R. Murray, R. F. Pease, J. F. Rablot, K. J. Wynne, and H. Yu, Langmuir **3**, 932 (1987).
[4] R. G. Nuzzo and D. L. Allara, J. Am. Chem. Soc. **105**, 4481 (1983).
[5] C. A. Goss, D. H. Charych, and M. Majda, Anal. Chem. **63**, 85 (1991).
[6] S. A. Joyce and J. E. Houston, Rev. Sci. Instrum. **62**, 710 (1991).
[7] K. B. Lodge, Adv. Coll. **19**, 27 (1983).
[8] N. A. Burnham and R. J. Colton, J. Vac. Sci. Technol. A **7**, 2906 (1989).
[9] E. W. Muller and T. T. Tsong, *Field Ion Microscopy* (American Elsevier, New York, 1969), Chap. IV.
[10] S. A. Joyce, R. C. Thomas, J. E. Houston, T. A. Michalske, and R. M. Crooks (unpublished).
[11] R. Erlandsson, G. Hadziioannou, C. M. Mate, G. M. McClelland, and S. Chiang, J. Chem. Phys. **89**, 5190 (1988).
[12] C. M. Mate, M. R. Lorenz, and V. J. Novotny, J. Chem. Phys. **90**, 7550 (1989).
[13] G. S. Blackman, C. M. Mate, and M. R. Philpott, Phys. Rev. Lett. **65**, 2270 (1990).

This article is copyrighted as indicated in the article. Reuse of AIP content is subject to the terms at: http://scitation.aip.org/termsconditions. Downloaded to IP: 129.22.67.107 On: Mon, 24 Nov 2014 07:35:14